

Prediction of cervical lymph node metastasis with contrast-enhanced ultrasound and association between presence of BRAF^{V600E} and extrathyroidal extension in papillary thyroid carcinoma

Jia Zhan* , Long-hui Zhang*, Qing Yu, Chao-lun Li, Yue Chen, Wen-Ping Wang and Hong Ding

Abstract

Objective: This study aimed to evaluate the correlation between cervical lymph node metastasis (CLNM) and each of the ultrasound features, immunohistochemical factors, and B-type Raf (BRAF^{V600E}) mutation.

Methods: A retrospective analysis was performed on 405 patients with single papillary thyroid carcinoma (PTC) nodules, all of whom underwent preoperative sonographic examinations, including gray-scale ultrasound, color Doppler ultrasound, and contrast-enhanced ultrasound (CEUS). All PTC patients were evaluated using 14 clinical and sonographic features, eight immunohistochemical factors, and BRAF^{V600E}. Multivariate analyses were performed to identify the risk factors for CLNM, and an equation for CLNM was established. The diagnostic value of each modality was compared with a receiver operating characteristic (ROC) curve.

Results: Among the 405 PTC nodules removed surgically, CLNM was confirmed in 138 patients, whereas extrathyroidal extension was confirmed in 185 patients. Multivariate analyses indicated significant differences between CLNM and non-CLNM groups in three conventional ultrasound features ($p < 0.05$), whereas other sonographic features, eight immunohistochemical factors, and BRAF^{V600E} did not indicate significant differences. A ROC curve of 0.757 in the equation exhibited a significant difference compared with the solo factors ($p < 0.05$ for all). Hyper or isoechoic enhancement at peak time on CEUS was associated with CLNM, whereas the presence of the BRAF^{V600E} mutation was associated with extrathyroidal extensions although BRAF appeared to be uncorrelated with CLNM in the present study.

Conclusion: Intensity at peak time, homogeneity, and size are the three most significant features in predicting CLNM in PTC patients, and the presence of the BRAF^{V600E} mutation was associated with extrathyroidal extensions when PTCs showed a hyper or isoechoic enhancement at peak time in CEUS.

Keywords: BRAF gene, contrast-enhanced ultrasound, extrathyroidal extension, lymph node metastasis, papillary thyroid carcinoma

Received: 2 March 2020; revised manuscript accepted: 19 June 2020.

Introduction

Papillary thyroid carcinoma (PTC), the most typical endocrine tumor,¹ has shown an increasing incidence over recent decades, with 7.8% in men

and 7.2% in women.² Most PTC patients have good prognoses; however, 30–40% of patients experience cervical lymph node metastasis (CLNM),³ which increases the risk of

Ther Adv Med Oncol

2020, Vol. 12: 1–13

DOI: 10.1177/
1758835920942367

© The Author(s), 2020.
Article reuse guidelines:
sagepub.com/journals-
permissions

Correspondence to:

Hong Ding
Department of Ultrasound,
Zhongshan Hospital,
Fudan University, Fenglin
Road No.180, Shanghai,
200032, P.R. China
ding.hong@zs-hospital.sh.cn

Jia Zhan
Department of Ultrasound,
Huadong Hospital, Fudan
University, Shanghai P.R.
China

Department of Ultrasound,
Zhongshan Hospital,
Fudan University,
Shanghai, P.R. China

Long-hui Zhang
Qing Yu
Chao-lun Li
Wen-Ping Wang
Department of Ultrasound,
Zhongshan Hospital,
Fudan University,
Shanghai, P.R. China

Yue Chen
Department of Ultrasound,
Huadong Hospital, Fudan
University, Shanghai P.R.
China

*These authors
contributed equally and
should be considered joint
first authors.



PTC recurrence and has been discovered to be associated with PTC-related deaths.⁴ Therapeutic central compartment node dissection has been recommended for PTC patients predisposed to CLNM;⁵ however, central compartment node dissection is not necessary for those with low-risk CLNM. In addition to central compartment node dissection, postsurgical radioiodine therapy is performed to eliminate aggressive PTCs.⁶ As the approach is detrimental to a patient's health, it is necessary to assess the risk factors of CLNM and establish a procedure to screen preoperatively for aggressive PTCs as part of the formulation of therapeutic strategies.

Recently, biological differences between PTCs have been discovered from the identification of genetic alterations in various signaling pathways.⁷ Among the genetic alterations, the B-type Raf (BRAF^{V600E}) kinase mutation on exon 15 is associated with the protein kinase pathway and contributes significantly to the initiation and progression of PTCs.⁸ Previous studies^{9,10} have reported a strong association between BRAF^{V600E} and the poor clinicopathological outcome of PTCs; however, a paradox has been observed between the high frequency of BRAF^{V600E} mutations in PTCs and the low prevalence of CLNM.^{11–13} Hence, controversy remains concerning the value and accuracy of BRAF in predicting CLNM.

Although the American Thyroid Association guidelines recommend ultrasound as the preferred imaging modality for the assessment of CLNM in PTC patients,¹⁴ previous studies discovered that preoperative conventional ultrasound missed 33–90% of CLNM in PTC patients.^{4,15} Instead of direct detection, researchers focused on the sonographic features of PTCs to predict CLNM, and conventional ultrasound features alone were ineffective for such a purpose.^{16,17} Hence, more advanced ultrasound devices are required to screen for aggressive PTCs from massive indolent ones and predict CLNM.

In recent years, contrast-enhanced ultrasound (CEUS) has been developed rapidly to predict the aggressiveness and prognosis of PTCs,¹⁸ and heterogeneous hypoechoic enhancement in thyroid nodules was discovered to be the most valuable parameter in predicting CLNM.¹⁹ Furthermore, CEUS was discovered to be significantly correlated with BRAF expression but not

directly with CLNM; however, BRAF overexpression was associated with CLNM.¹⁸

In addition to genes, many immunohistochemical markers have been discovered to be correlated with PTCs, such as neural cell adhesion molecule (CD56), cytokeratin 19 (CK19), Galectin-13, Hector Battifora mesothelial-1 (HBME-1), Ki-67, mesenchymal-epithelial transition factor (Met), thyroglobulin (TG), and thyroid peroxidase (TPO),^{20–22} However, the association between immunohistochemical markers and CLNM in PTC remains unclear.

The present study aimed to investigate the relationship between CLNM and each of the ultrasound features, CEUS features, immunohistochemical markers, and BRAF expressions of PTCs.

Materials and methods

Patients

A retrospective analysis was performed in patients undergoing thyroid nodule work-up in the Zhongshan Hospital in Shanghai from January 2017 to October 2018. The inclusion criteria were as follows: (a) adults older than 18 years; (b) patients have received fine needle aspiration (FNA) with the Bethesda System for Reporting Thyroid Cytopathology category V or VI (most patients with nodules smaller than 1 cm received FNA in other hospitals because they were worried about canceration); (c) patients have nodules larger than 0.5 cm (with nodules smaller than 0.5 cm, it is difficult to maintain the same imaging sections during CEUS because of arterial pulsations and breathing); (d) patients have received a partial (lobectomy or near total thyroidectomy) or a total thyroidectomy coupled with a central lymph node dissection (level VI) in the presence of clinical or ultrasound evidence of lymph node involvement. Lateral neck dissection is recommended during thyroidectomy based on clinical findings if CLNMs have been discovered in other imaging studies. The extent of thyroid surgery was determined mainly in accordance with the American Thyroid Association guidelines. The exclusion criteria were as follows: (a) PTC with coarse calcifications; (b) nodules histopathologically confirmed to be benign (false-positive FNA); (c) patients with multiple nodules confirmed to be PTC (in cases of multiple and bilateral PTC nodules, the thyroid nodule

causing CLNM is difficult to identify); (d) pregnant women.

Among 550 patients who underwent preoperative conventional ultrasound and CEUS for thyroid nodules, 145 of them were excluded because partial immunohistochemical markers were missing; therefore, 405 nodules were discovered in 405 patients (109 men and 296 women, aged 18–81 years with an average age of 46.1 ± 12.4) in this prospective study.

Conventional ultrasound grayscale and color Doppler ultrasound

All ultrasonographic studies were performed using machines from four vendors: a Philips iU22 (Bothell, WA, USA) equipped with a L12-5 transducer for conventional ultrasound and a L9-3 for CEUS; a LOGIQ E9 (GE Healthcare, Chalfont St Giles, UK) equipped with a ML6-15 transducer for conventional ultrasound and a 9L for CEUS; an Apoli 500 (Toshiba, Tokyo, Japan) equipped with a 14L5 transducer for conventional ultrasound and CEUS; and a S2000 (Siemens, Germany) equipped with a 9L4 transducer for conventional ultrasound and CEUS. The patients were in the supine position with a dorsal flexion of the head. Conventional ultrasound was performed by experienced examiners.

Using grayscale ultrasound, thyroid nodules were evaluated based on the interior echogenicity, with nodules classified as hyperechoic, isoechoic, or hypoechoic relative to normal thyroid parenchyma, shape (regular or irregular), margin (well or poorly defined), orientation (wider than tall, or taller than wide), and presence or absence of microcalcification (hyperechoic spots less than 1 mm without acoustic shadowing in solid tissues).

Color Doppler ultrasound was performed after grayscale ultrasound. The PTCs were examined for vascular distribution and classified into three patterns: (a) none; (b) perinodular and absence of or slight intranodular blood flow; (c) abundant intranodular and absence of or slight perinodular blood flow.²³

Contrast-enhanced ultrasound

The largest nodule was selected on the conventional ultrasound before the transducer was

switched to CEUS mode. For comparability, the focus zone was always set at the bottom of the nodule. CEUS was performed using low mechanical index imaging ($MI < 0.10$) to minimize microbubble destruction and artificial signal loss. A 1.5 mL contrast agent (SonoVue, Bracco International, Milan, Italy) was injected intravenously as a bolus, followed by a 5 mL saline flush (0.9% sodium chloride). The timer on the ultrasound device was started during CEUS, and imaging lasting at least 2 min was stored digitally as raw data.

The thyroid nodules were evaluated on CEUS relative to normal thyroid parenchyma. The appearance of microbubbles was classified as earlier than adjacent thyroid parenchyma or the bubbles appear in thyroid nodule meantime as surrounding; meanwhile, peak intensity was classified as hyper, iso, or hypoechoic enhancement and compared with adjacent thyroid parenchyma at the peak time (Figure 1). A homogeneous enhancement was defined as an occupation with a full enhancement of the contrast agent, regardless of the enhancement degree. A heterogeneous enhancement was defined as an enhanced lesion with areas without enhancement. The enhancement pattern was defined as a centripetal enhancement, that is, an enhancement from a lesion periphery to the center. A comprehensive enhancement occurred when both the peripheral and central areas of the lesion were enhanced synchronously.

CEUS videos were retrospectively reviewed by two observers (JZ and XHD) who were blinded to each other's judgment. Discrepancies were adjudicated by discussions with a third reviewer (HD). Sensitivity, specificity, and area under the receiver operating characteristic curve were calculated independently.

Histological and immunohistochemical analysis

All surgical specimens were categorized according to the World Health Organization histological classification of thyroid tumors (2003)²⁴ by experienced pathologists who were blinded to the medical history and ultrasonographic findings. Pathological diagnosis was considered as the gold standard for the study.

Immunohistochemical assays were performed for CD56, CK19, galectin-13, HBME-1, Ki-67, Met, TG, and TPO. Tissue sections were deparaffinized and rehydrated in xylene to reduce alcohol

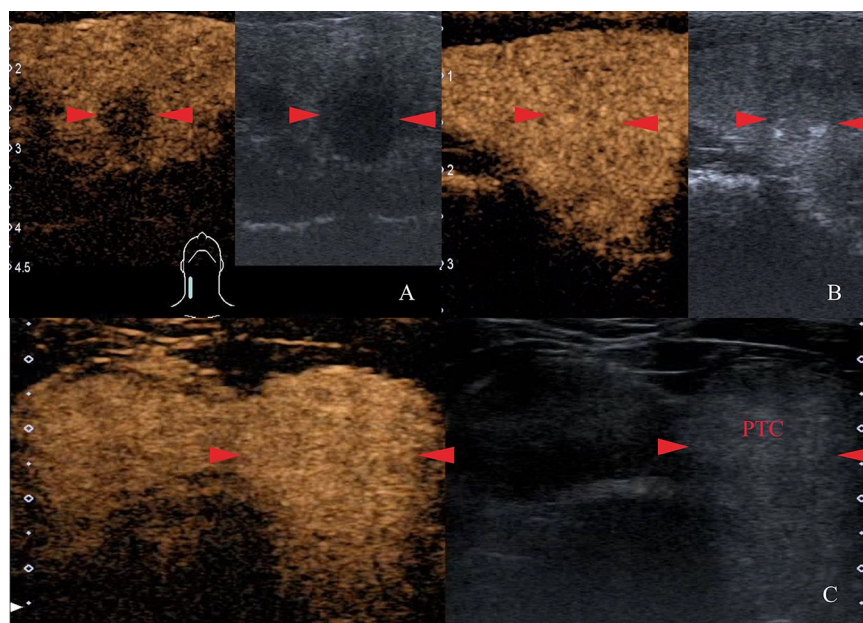


Figure 1. Representative images of degree of enhancement at peak time on CEUS. (A) The PTC (red arrows) enhances heterogeneously to a lower degree (anechoic defects) than normal thyroid parenchyma at peak time. (B) The PTC (red arrows) occupied by a full enhancement of contrast agent, and it is difficult to distinguish from normal thyroid parenchyma. (C) The PTC enhances homogeneously to a higher degree (brighter) than normal thyroid parenchyma at peak time. CEUS, contrast-enhanced ultrasound; PTC, papillary thyroid carcinoma.

dilutions. Immunohistochemistry was performed on tissue microarray (TMA) sections of 3 mm in an automated Leica Bond III stainer for CD56 (product ID: NCL-CD56-1B6, clone: 1B6), CK-19 (product ID: M0342, clone: K19.2), HBME-1 (product ID: MAB-0130, clone: HBME1), galectin-13 (product ID: NCL-L-GAL3, clone: 9C4), Ki-67 (product ID: M7240, clone: M1B1), Met (product ID: 8198S, clone: D1C2), TG (product ID: M-0495, clone: SPM517), and TPO (product ID: MAB-0630, clone: AC25).

BRAF mutation analysis

The BRAF^{V600E} mutation was analyzed in the Pathology Department of Zhongshan Hospital. The DNA of surgically obtained tissue samples was extracted using a Qiagen QIA amp DNA FFPE tissue kit (56404, Qiagen) in 50 mL of buffer ATE (part of the kit) based on the manufacturer's protocol. The absorbance of the extracted DNA was tested using a Merinton SMA 4000 spectrophotometer (Merinton Inc., Beijing, China). BRAF exon 15 was amplified

by polymerase chain reaction (forward: TCATAATGCTTGCTCTGATAGGA, reverse: GGCCAAAATTTAA TCAGTGGA).

Statistical analysis

Patients were categorized into groups according to nodule size, enhancement pattern, and presence of CLNM. Continuous quantitative data were expressed as mean \pm standard deviation. The χ^2 test was employed to compare the categorical variables of clinical features, whereas the Cochran–Mantel–Haensel χ^2 test was performed to analyze stratified or matched categorical data. A multivariate logistic regression was performed to determine the independent factors associated with CLNM. Odds ratios (ORs) with 95% confidence intervals were calculated and receiver operating characteristic (ROC) curves were generated for factors with significance in the multivariate logistic regression. The kappa values were calculated to assess the inter-observer agreement of CEUS features between different radiologists.

All statistical tests were performed using commercially available software (Stata, version 10.0;

Stata Corp, College Station, TX, USA). For all tests, $p < 0.05$ was considered indicative of statistical significance.

Results

Histological findings

Histopathologically, 405 patients were diagnosed as PTC patients having only one carcinoma measuring 8.8 ± 3.2 mm (range: 5–35.0 mm). CLNM was discovered in 138 (34.1%) patients (Figure 2) and extrathyroidal extension was performed on 185 patients (45.7%) (Figure 3). Among those with CLNM, 102 patients (25.2%) had central lymph node metastasis (LNM), 16 (4.0%) had lateral LNM, and 20 (4.9%) had both. All tumor samples were successfully genotyped for BRAF^{V600E} and eight immunohistochemical markers.

Important features in conventional ultrasound and CEUS

The gender, size, taller-than-wide shape, peak intensity, and homogeneity in CEUS differed significantly between patients with and without CLNM ($p < 0.05$, Table 1). However, the mean age, location, margin, shape, echogenicity, microcalcification in nodules, Color Doppler flow imaging (CDFI) patterns, earlier arrival, and enhancement pattern were not statistically significantly different between the two groups ($p > 0.05$) (Table 1). The BRAF^{V600E} mutation and all immunohistochemical markers in our study had no correlation with CLNM (Table 2).

Inter-observer variability of CEUS features

The kappa values of four CEUS features between two radiologists ranged from 0.540 to 0.765, and all p values of kappa were 0.000 (Table 3).

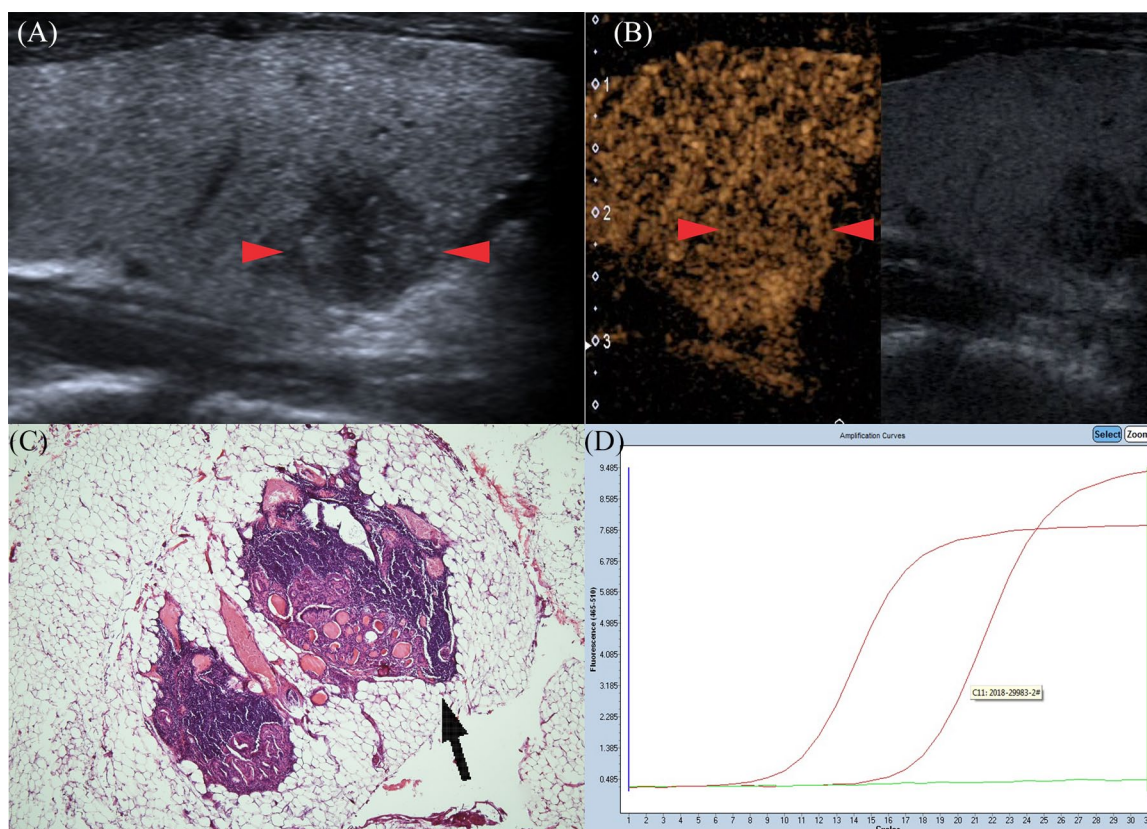


Figure 2. Gray-scale ultrasonography features of PTC in a 24-year-old man (red arrows): round shape; not well defined; hypoechoic in interior echogenicity. (A) CEUS features of PTC (red arrows): the nodule shows homogeneous iso-enhancement at peak time compared with normal thyroid parenchyma. (B) Pathological examination confirmed the diagnosis of CLNM (black arrow), also with ETE (HE hematoxylin and eosin stain $\times 40$) (C). Amplification plot of PTC with BRAF^{V600E} mutation (D). CEUS, contrast-enhanced ultrasound; CLNM, cervical lymph node metastasis; ETE, extrathyroidal extension; PTC, papillary thyroid carcinoma.

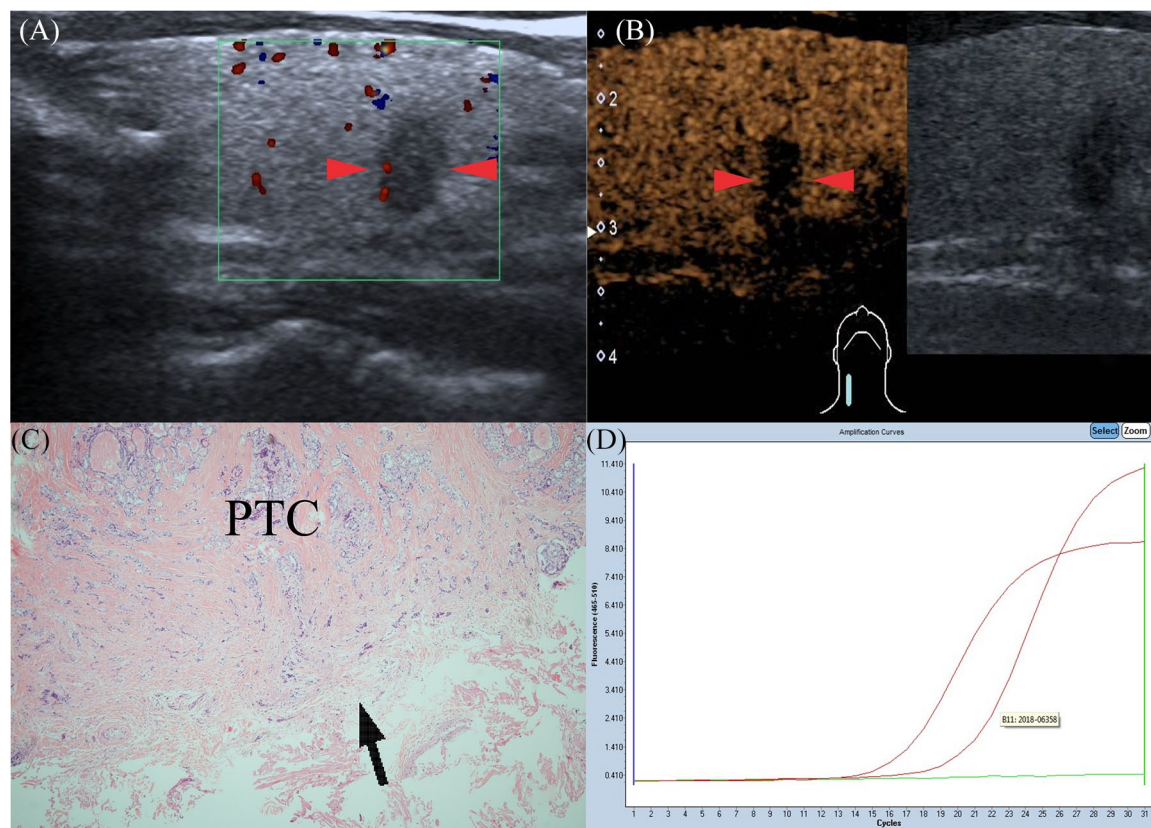


Figure 3. Gray-scale ultrasonography features of PTC in a 41-year-old man (red arrows): taller than wide; not well-defined; hypoechoic in interior echogenicity. (A) CEUS features of PTC (red arrows): the nodule shows heterogeneous hypo-enhancement at peak time compared with normal thyroid parenchyma. (B) Pathological examination confirmed the diagnosis of PTC with ETE (black arrow), but without CLNM (HE \times 40) (C). Amplification plot of PTC with BRAF^{V600E} mutation (D). CEUS, contrast-enhanced ultrasound; CLNM, cervical lymph node metastasis; ETE, extrathyroidal extension; PTC, papillary thyroid carcinoma.

Multivariate logistic regression

Multivariate logistic regression was performed for all significant variables. The three most important predictive factors were intensity at peak time (OR = 4.733, $p = 0.000$), homogeneity (OR = 2.18, $p = 0.030$), and size (OR = 2.16, $p = 0.003$), whereas the others were dependent on CLNM ($p > 0.05$) (Table 4). The areas under the ROC curves were 0.703 for intensity at peak time [95% confidence interval (CI): 0.657–0.701], 0.560 for homogeneity (95% CI: 0.519–0.600), and 0.598 for size (95% CI: 0.545–0.650), respectively.

An equation was created for multivariate logistic regression with the three most significant predictive factors: $p = 1/1 + \exp \Sigma [-1.612 + 2.16 \times \text{size} + 2.18 \times \text{homogeneity} + 6.58 \times \text{Intensity at peak time}]$. The equation area under the ROC curve of 0.757 (95% CI: 0.707–0.807) indicated a significant difference compared with the three solo factors ($p < 0.05$ for all) (Figure 4).

The predictive equation indicated the highest sensitivity (67.4%) in predicting CLNM, whereas CEUS homogeneity indicated the highest specificity (88.0%). The diagnostic accuracy of the prediction from the predictive equation was 74.8% (Table 5).

Association of CEUS features and BRAF^{V600E} mutation with pathological data

An investigation of the CEUS features and pathological characteristics of PTC revealed that, in the presence of the BRAF^{V600E} mutation, hyper or isoechoic enhancement at peak time in CEUS was associated with male patients ($p = 0.006$), PTC size ($p = 0.001$), CLNM ($p = 0.000$); and in the absence of the BRAF^{V600E} mutation, it was associated with the number of lymph nodes harvested ($p = 0.025$) and involved ($p = 0.000$) as well as CLNM ($p = 0.001$). The absence of the BRAF^{V600E} mutation was associated with the

Table 1. Basic patients' characteristics and conventional ultrasound features of papillary thyroid carcinoma (PTC).

Indicators	Total PTCs with CLNM (n = 405)		p value
	Yes (n = 138)	No (n = 267)	
Mean age	43.0 ± 1.09	47.7 ± 0.73	0.14
Age range	18–81	23–78	
Gender			0.025
Male	47 (34.1%)	62 (23.2%)	
Female	91 (65.9%)	205 (76.8%)	
Size			0.001
<10 mm and ≥5 mm	66 (47.8%)	175 (65.5%)	
<20 mm and ≥10 mm	55 (39.9%)	80 (30.0%)	
≥20 mm	17 (12.3%)	12 (4.5%)	
Location			0.155
Left	69 (50.0%)	124 (46.4%)	
Right	66 (47.8%)	142 (53.2%)	
Isthmus	3 (2.2%)	1 (0.4%)	
Lymph-vascular/neural invasion			0.096
Yes	6 (4.3%)	4 (1.5%)	
No	132 (95.7%)	263 (98.5%)	
Shape			0.674
Regular	83 (60.1%)	161 (60.3%)	
Irregular	55 (39.9%)	106 (39.7%)	
Margin			0.855
Well defined	44 (31.9%)	109 (40.8%)	
Poorly defined	94 (68.1%)	158 (59.2%)	
Echogenicity			0.453
Hypoechoic	128 (92.8%)	255 (95.5%)	
Isoechoic	6 (4.3%)	6 (2.4%)	
Hyperechoic	4 (2.9%)	6 (2.4%)	0.021

*(Continued)***Table 1.** (Continued)

Indicators	Total PTCs with CLNM (n = 405)		p value
	Yes (n = 138)	No (n = 267)	
Taller than wide			
Yes	83 (60.1%)	128 (47.9%)	
No	55 (39.9%)	139 (52.1%)	0.284
Calcification			
Microcalcification	60 (43.5%)	100 (37.5%)	
No calcification	78 (56.5%)	167 (62.5%)	0.182
CDFI patterns			
Type I	51 (37.0%)	111 (41.6%)	
Type II	77 (55.8%)	147 (55.1%)	
Type III	10 (7.2%)	9 (3.3%)	0.196
Earlier arrival on CEUS			
Earlier	6 (4.3%)	5 (1.9%)	
Meantime	132 (95.6%)	262 (98.1%)	0.000
Peak intensity on CEUS			
Hypoechoic enhancement	59 (42.8%)	221 (82.8%)	
Isoechoic enhancement	66 (47.8%)	39 (14.6%)	
Hyperechoic enhancement	13 (9.4%)	7 (2.6%)	
Homogeneity on CEUS			0.003
Heterogeneous	33 (23.9%)	32 (11.9%)	
Homogeneous	105 (76.1%)	235 (88.1%)	
CEUS enhancement pattern			0.608
Centripetal	2 (1.4%)	2 (0.7%)	
Entire	136 (98.6%)	265 (99.3%)	

CDFI, Color Doppler flow imaging; CEUS, contrast-enhanced ultrasound; CLNM, cervical lymph node metastasis; PTC, papillary thyroid carcinoma.

Table 2. Immunohistochemistry and BRAF mutation analysis for the patients with PTCs.

Indicators	Total PTCs with CLNM (n=405)		p value
	Yes (n=138)	No (n=267)	
CD56			0.396
Positive	63 (45.7%)	109 (40.8%)	
Negative	75 (54.3%)	158 (59.2%)	
CK19			1.000
Positive	136 (98.6%)	263 (98.5%)	
Negative	2 (1.4%)	4 (1.5%)	
Galectin-13			0.830
Positive	129 (93.5%)	251 (94.0%)	
Negative	9 (6.5%)	16 (6.0%)	
HBME-1			0.200
Positive	105 (76.1%)	186 (69.7%)	
Negative	33 (23.9%)	81 (30.3%)	
Ki-67			0.347
Positive	137 (99.3%)	267 (100%)	
Negative	1 (0.7%)	0 (0%)	
Met			0.414
Positive	135 (97.8%)	264 (98.9%)	
Negative	3 (2.2%)	3 (1.1%)	
TG			1.000
Positive	136 (98.6%)	263 (98.5%)	
Negative	2 (1.4%)	4 (1.5%)	
TPO			0.461
Positive	84 (60.9%)	158 (59.2%)	
Negative	54 (39.1%)	120 (40.8%)	
BRAF gene			0.385
Positive	110 (79.7%)	202 (75.7%)	
Negative	28 (20.3%)	65 (24.3%)	

CD56, cell adhesion molecule; CK19, cytokeratin 19; CLNM, cervical lymph node metastasis; HBME, Hector Battifora mesothelial-1; Met, mesenchymal-epithelial transition factor; PTC, papillary thyroid carcinoma; TG, thyroglobulin; TPO, thyroid peroxidase.

number of lymph nodes involved ($p=0.0049$), whereas the presence of the BRAF^{V600E} mutation was associated with extrathyroidal extension when PTC showed hyper or isoechoic enhancement at peak time in CEUS (Table 6).

Discussion

Conventional ultrasound is important in the diagnosis of PTC. Solidness, irregular shapes, poorly defined margins, hyper-echogenicity, calcification, and taller-than-wide shapes are suspicious sonographic features although beneficial in predicting malignancy.^{25,26} However, we discovered that these conventional sonographic features did not perform well in predicting CLNM in the study. Therefore, complementary modalities are necessary for a more efficient diagnosis.

CEUS, which shows microvascular blood flow in tumors clearly, can be used to evaluate accurately the intensity of tumor perfusion and vascularity.^{27,28} As angiogenesis is fundamental in the development, growth, and metastasis of PTC, it was hypothesized in a previous study²⁹ that the larger the size of a PTC and the greater the enhancements at peak time, the greater is the microvascular density in the tumor tissue and the greater is the possibility of CLNM. As PTC develops further, malignancy infiltration causes neovascular damage, and perfusion defects within lesions are often observed in heterogeneous enhancements.¹⁹ Therefore, CLNM was reported to be correlated with hyper or isoechoic enhancements at peak time in CEUS, heterogeneous enhancement, and PTC size. A multivariate analysis coupled with CEUS findings revealed that an area under the ROC curve of 0.757 predicted CLNM in PTC patients, and it was a clearer indicator than other solo risk factors.

The BRAF mutation is a typical genetic alteration that results in the transformation of the valine of the BRAF protein 600-bit codon to glutamate, the abnormal proliferation of cells, and the formation of tumor. Studies showed that BRAF is the most important diagnostic value for PTC, with an approximately 73.4% mutation rate. Some studies have suggested that, based on a significant difference between CLNM (92.9%) and non-CLNM groups (78.6%), BRAF mutations in PTCs can result in higher aggressiveness,¹⁷ which was not shown in our study. Accordingly, it appears that the BRAF mutation is not a prognostic factor for PTC.

Histology serves as the gold diagnostic standard for CLNM. Several studies have confirmed the role of immunohistochemistry and a few molecular markers in the diagnosis of PTC.^{20–22} However, the use of those markers in predicting CLNM or prognosis remains controversial. In this present

Table 3. Inter-observer variability for CEUS features between two radiologists.

Observer 1		Observer 1		Observer 1		Observer 1	
Arrival time	Peak intensity	Homogeneity	Enhancement pattern	Arrival time	Peak intensity	Homogeneity	Enhancement pattern
Observer 2 Earlier	Observer 2 Hypoechoic	Observer 2 Heterogeneous	Observer 2 Centripetal	Observer 2 Earlier	Observer 2 Hypoechoic	Observer 2 Heterogeneous	Observer 2 Centripetal
15	264	50	2	15	264	50	2
Mean time 4	Mean time 9	Mean time 20	Mean time 3	Mean time 4	Mean time 9	Mean time 20	Mean time 3
380	380	320	398	380	380	320	398
k=0.737 p=0.000		k=0.540 p=0.000		k=0.694 p=0.000		k=0.765 p=0.000	
CEUS, contrast-enhanced ultrasound.							

Table 4. Multivariate logistic regression for predicting CLNM.

Overall (n=405)	B	Odds ratios	Err	95% CIs	p value
Size	2.16	1.561	0.321	1.043–2.337	0.030
Homogeneity	2.18	2.052	0.677	1.074–3.918	0.030
Intensity at peak time	6.58	4.773	1.089	3.052–7.464	0.000

CI, confidence interval; CLNM, cervical lymph node metastasis.

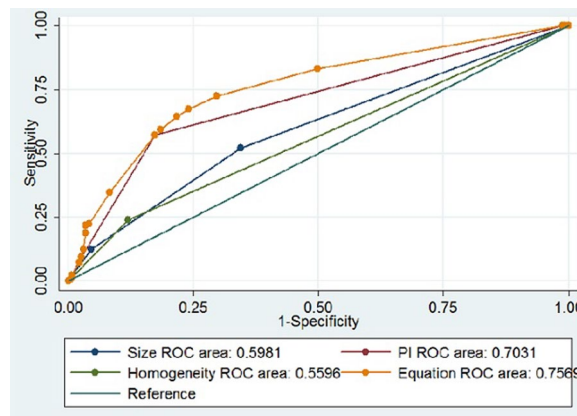


Figure 4. ROC curves of PTC size [area under the ROC curve (AUROC)=0.598], homogeneity on CEUS (AUROC=0.560), peak intensity on CEUS (AUROC=0.703), and Equation (AUROC=0.757) for the prediction of CLNM. CEUS, contrast-enhanced ultrasound; CLNM, cervical lymph node metastasis; PTC, papillary thyroid carcinoma; ROC, receiver operating characteristic.

study, no significant differences were observed between CLNM and non-CLNM groups in the eight immunohistochemical markers. Similar to BRAF, a high false-positive rate limits their application in predicting CLNM in PTC.

However, we discovered that the BRAF^{V600E} mutation was an independent influencing factor for extrathyroidal extension, as reported previously.^{30,31} Minimal extrathyroidal extension is identified by involvement of the sternothyroid muscle or perithyroid soft tissue, and is generally identified by light microscope examination in this study. The observation was applicable only when the PTC was iso or hyperechoic and the BRAF^{V600E} mutation had a weak association with extrathyroidal extension in hypoechoic cases, which may be attributed to rich blood supplies strengthening the genetic influence on extrathyroidal extension.

Table 5. ROC analysis for predicting CLNM in PTCs.

Overall (n=405)	Az	95% CIs	Sensitivity	Specificity	Accuracy
Size	0.598	0.546–0.650	52.2%	65.5%	61.0%
Homogeneity	0.560	0.519–0.600	23.9%	88.0%	66.2%
Intensity at peak time	0.703	0.657–0.751	57.3%	82.8%	74.1%
Predictive equation	0.757	0.707–0.807	67.4%	76.0%	74.8%

CI, confidence interval; CLNM, cervical lymph node metastasis; PTC, papillary thyroid carcinoma; ROC, receiver operating characteristic.

Table 6. Association of *BRAF* gene mutations/CEUS features with clinical characteristics of PTC patients.

Characteristics	<i>BRAF</i> +/ CEUS+(1)	<i>BRAF</i> +/ CEUS-(2)	<i>BRAF</i> -/ CEUS+(3)	<i>BRAF</i> -/ CEUS-(4)	<i>p</i> value	<i>p</i> value	<i>p</i> value	<i>p</i> value
	n=98	n=214	n=27	n=66	1 versus 2	3 versus 4	1 versus 3	2 versus 4
Age	45.2 ± 1.37	47.4 ± 0.83	43.1 ± 2.12	44.3 ± 1.44	0.162	0.643	0.459	0.107
Gender (F/M)	63/35	160/54	21/6	52/14	0.006	1.000	0.056	0.623
Size (B/M/S)	13/46/39	13/71/130	0/10/17	3/15/48	0.001	0.229	0.229	0.208
Location (L/R/I)	51/44/3	95/118/1	14/13/0	33/33/0	0.057	0.871	0.645	0.637
ETE (Y/N)	52/46	99/115	6/21	28/38	0.275	0.096	0.005	0.672
CLNM (Y/N)	65/33	45/169	14/13	14/52	0.000	0.006	0.183	1.000
No of LNs harvested	4.2 ± 0.4	3.1 ± 0.3	3.5 ± 0.6	3.2 ± 0.5	0.025	0.733	0.407	0.886
No. of LNs involved	1.7 ± 0.2	0.5 ± 0.1	1.1 ± 0.3	0.5 ± 0.2	0.000	0.049	0.111	0.844

B/M/S, big/middle/small; CEUS+, hyper or isoechoic enhancement at peak time on CEUS; CEUS-, hypo enhancement at peak time on CEUS; CLNM, cervical lymph node metastasis; ETE, extrathyroidal extension; F/M, female/male; LNs, lymph nodes; L/R/I, left/right/isthmus; PTC, papillary thyroid carcinoma.

Our study was substantial in several respects. First, we used a sample larger than those of previous studies. Second, our study involved a wide coverage including 14 clinical and ultrasound features, eight immunohistochemical factors, and the *BRAF*^{V600E} mutation to predict not only CLNM, but also extrathyroidal extension. Third, we investigated the association between CEUS and CLNM, as many studies^{32–34} claimed that *BRAF* did not contribute to the prediction of CLNM. Finally, the exclusion of multiple and bilateral PTCs confirmed that PTCs resulted in CLNM.

However, the current study has some limitations. First, we did not use long-term follow-up data

with a median follow-up duration of 13 months (range: 3–24 months). More CLNMs may occur after the follow-up. Second, CLNMs were histologically confirmed, and CLNM detection in the current study was limited without other radiological examinations. Enhanced computed tomography (CT) and the use of quantitative parameters derived from multiphase CT significantly improved the accuracy in detecting CLNMs from PTC.^{35–37} Third, a selection bias may be caused by the inclusion of solo PTCs. Moreover, in view of the large sample, thyroid ultrasonography was performed by more than one person in the study which may also cause bias. Finally, only *BRAF* was included, and more

genes such as TERT and RAS may be analyzed in the future.

In conclusion, the size, intensity at peak time, and homogeneity in CEUS are predictors of risk for CLNM in PTC. The model equation created in our study can steadily predict the risk of CLNM; therefore, it might be useful for the prognosis of and formulating appropriate strategies for PTC and avoiding second central compartment node dissection.

Acknowledgements

This paper was edited by Professor Qingxiang Sun who was Director of Medical English Center (MEC), College of Foreign Languages and Literature, Fudan University; visiting scholar of California State University, Fullerton.

Conflict of interest statement

The authors declare that there is no conflict of interest.

Funding

The authors disclosed receipt of the following financial support for the research, authorship, and/or publication of this article: This study was funded by the Medical Guide Project of the Shanghai Science and Technology Commission (grant No.14411970400).

Ethics statement

The study was performed in accordance with the ethical guidelines of the Declaration of Helsinki and approved by the ethics committee of the Zhongshan Hospital Fudan University (approval number: B2012-105).

This article does not contain any studies with animals performed by any of the authors.


All procedures performed in studies involving human participants were in accordance with the ethical standards of the institutional and/or national research committee and with the 1964 Declaration of Helsinki and its later amendments or comparable ethical standards.

Informed consent

Informed consent was obtained from all individual participants included in the study. The informed consent included: (1) patient's diagnosis; (2) the procedure that the radiologists recommend; (3) risks and benefits of the procedure; (4) the potential side effects of contrast agent injection. Signing informed consent means: (1) you have been well informed about CEUS by the

radiologist; (2) you understand the information and you have had a chance to ask questions; (3) you use this information to decide if you want to receive the CEUS procedure; (4) if you agree to receive CEUS, you give your consent (agree) by signing a consent form. The completed and signed form is a legal document that lets your radiologist go ahead with the examination.

ORCID iD

Jia Zhan  <https://orcid.org/0000-0002-2179-4095>

References

1. Pellegriti G, Frasca F, Regalbuto C, *et al.* Worldwide increasing incidence of thyroid cancer: update on epidemiology and risk factors. *J Cancer Epidemiol* 2013; 2013: 965212.
2. Colonna M, Uhry Z, Guizard A, *et al.* Recent trends in incidence, geographical distribution, and survival of papillary thyroid cancer in France. *Cancer Epidemiol* 2015; 39: 511–518.
3. Spios JA. Advances in ultrasound for the diagnosis and management of thyroid cancer. *Thyroid* 2009; 19: 1363–1372.
4. Baek SK, Jung SY, Kang SM, *et al.* Clinical risk factors associated with cervical lymph node recurrence in papillary thyroid carcinoma. *Thyroid* 2010; 20: 147–152.
5. Haugen BR, Alexander EK, Bible KC, *et al.* 2015 American Thyroid Association management guidelines for adult patients with thyroid nodules and differentiated thyroid cancer: the American Thyroid Association guidelines task force on thyroid nodules and differentiated thyroid cancer. *Thyroid* 2016; 26: 1–133.
6. Luster M, Aktolun C, Amendoeira I, *et al.* European perspective on 2015 American Thyroid Association management guidelines for adult patients with thyroid nodules and differentiated thyroid cancer: proceedings of an interactive international symposium. *Thyroid* 2019; 29: 7–26.
7. Lee MY, Ku BM, Kim HS, *et al.* Genetic alterations and their clinical implications in high-recurrence risk papillary thyroid cancer. *Cancer Res Treat* 2016; 49: 906–914.
8. Xing M. Molecular pathogenesis and mechanisms of thyroid cancer. *Nat Rev Cancer* 2013; 13: 184–199.
9. Lee JH, Lee ES and Kim YS. Clinicopathologic significance of BRAF^{V600E} mutation in papillary carcinomas of the thyroid: a meta-analysis. *Cancer* 2010; 110: 38–46.

10. Jung CK, Choi YJ, Lee KY, *et al.* The cytological, clinical, and pathological features of the cribriform-morular variant of papillary thyroid carcinoma and mutation analysis of CTNNB1 and BRAF genes. *Thyroid* 2009; 19: 905–913.
11. Celik M, Bulbul BY, Ayturk S, *et al.* The relation between BRAF^{V600E} mutation and clinicopathological characteristics of papillary thyroid cancer. *Med Glas (Zenica)* 2020; 17: 30–34.
12. Özçelik S, Bircan R, Sarıkaya Ş, *et al.* BRAF^{V600E} mutation in papillary thyroid cancer is correlated with adverse clinicopathological features but not with iodine exposure. *Endokrynol Pol* 2019; 70: 401–408.
13. Sezer A, Celik M, Yilmaz Bulbul B, *et al.* Relationship between lymphovascular invasion and clinicopathological features of papillary thyroid carcinoma. *Bosn J Basic Med Sci* 2017; 17: 144–151.
14. Cooper DS, Doherty GM, Haugen BR, *et al.* Revised American Thyroid Association management guidelines for patients with thyroid nodules and differentiated thyroid cancer. *Thyroid* 2009; 19: 1167–1214.
15. Moo TA, McGill J, Allendorf J, *et al.* Impact of prophylactic central neck lymph node dissection on early recurrence in papillary thyroid carcinoma. *World J Surg Oncol* 2010; 34: 1187–1191.
16. Xu JM, Xu XH, Xu HX, *et al.* Prediction of cervical lymph node metastasis in patients with papillary thyroid cancer using combined conventional ultrasound, strain elastography, and acoustic radiation force impulse (ARFI) elastography. *Eur Radiol* 2016; 26: 2611–2622.
17. Chen J, Li XL, Zhao CK, *et al.* Conventional ultrasound, immunohistochemical factors and BRAF^{V600E} mutation in predicting central cervical lymph node metastasis of papillary thyroid carcinoma. *Ultrasound Med Biol* 2018; 44: 2296–2306.
18. Wei X, Li Y, Zhang S, *et al.* Prediction of thyroid extracapsular extension with cervical lymph node metastases (ECE-LN) by CEUS and BRAF expression in papillary thyroid carcinoma. *Tumor Biol* 2014; 35: 8559–8564.
19. Zhang Y, Luo YK, Zhang MB, *et al.* Values of ultrasound features and MMP-9 of papillary thyroid carcinoma in predicting cervical lymph node metastases. *Sci Rep* 2017; 7: 6670.
20. Can N, Tastekin E, Ozyilmaz F, *et al.* Histopathological evidence of lymph node metastasis in papillary thyroid carcinoma. *Endocr Pathol* 2015; 26: 218–228.
21. Park YJ, Kwak SH, Kim DC, *et al.* Diagnostic value of Galectin-3, HBME-1, Cytokeratin 19, high molecular weight cytokeratin, Cyclin D1 and p27kip1 in the differential diagnosis of thyroid nodules. *J Korean Med Sci* 2007; 22: 621–628.
22. Cho H, Kim JY and Oh YL. Diagnostic value of HBME-1, CK19, Galectin 3, and CD56 in the subtypes of follicular variant of papillary thyroid carcinoma. *Pathol Int* 2018; 68: 605–613.
23. Rago T, Vitti P, Chiovato L, *et al.* Role of conventional ultrasonography and color flow-doppler sonography in predicting malignancy in ‘cold’ thyroid nodules. *Eur J Endocrinol* 1998; 138: 41–46.
24. Delellis RA. Tumors of the thyroid and parathyroid. In: Delellis RA (ed) *World Health Organization classification of tumors: pathology and genetics of tumors of endocrine organs*. IARC Press, Lyon, France, 2004, pp. 49–133.
25. Gharib H, Papini E, Paschke R, *et al.* American association of clinical endocrinologists, Associazione Medici Endocrinologi, and European thyroid association medical guidelines for clinical practice for the diagnosis and management of thyroid nodules: executive summary of recommendations. *Endocr Pract* 2010; 16: 468–475.
26. Kwak JY, Han KH, Yoon JH, *et al.* Thyroid imaging reporting and data system for US and features of nodules: a step in establishing better stratification of cancer risk. *Radiology* 2011; 260: 892–899.
27. Piscaglia F1, Nolsøe C, Dietrich CF, *et al.* The EFSUMB guidelines and recommendations on the clinical practice of contrast enhanced ultrasound (CEUS): update 2011 on non-hepatic applications. *Ultraschall Med* 2012; 33: 33–59.
28. Bertolotto M and Catalano O. Contrast-enhanced ultrasound: past, present, and future. *Ultrasound Clin* 2009; 4: 339–367.
29. Zhan J, Diao XH, Chen Y, *et al.* Predicting cervical lymph node metastasis in patients with papillary thyroid cancer (PTC) - why contrast-enhanced ultrasound (CEUS) was performed before thyroidectomy. *Clin Hemorheol Microcirc* 2019; 72: 61–73.
30. Moon HJ, Kim EK, Chung WY, *et al.* Minimal extrathyroidal extension in patients with papillary thyroid microcarcinoma: is it a real prognostic factor? *Ann Surg Oncol* 2011; 18: 1916–1923.

31. Ren H, Shen Y, Hu D, *et al.* Co-existence of BRAF^{V600E} and TERT promoter mutations in papillary thyroid carcinoma is associated with tumor aggressiveness, but not with lymph node metastasis. *Cancer Manag Res* 2018; 10: 1005–1013.
32. Han PA, Kim HS, Cho S, *et al.* Association of BRAF(V600E) mutation and microrna expression with central lymph node metastases in papillary thyroid cancer: a prospective study from four endocrine surgery centers. *Thyroid* 2016; 26: 532–542.
33. Li C, Aragon Han P, Lee KC, *et al.* Does BRAF^{V600E} mutation predict aggressive features in papillary thyroid cancer? Results from four endocrine surgery centers. *J Clin Endocrinol Metab* 2013; 98: 3702–3712.
34. Liu C, Chen T and Liu Z. Associations between BRAF^{V600E} and prognostic factors and poor outcomes in papillary thyroid carcinoma: a meta-analysis. *World J Surg Oncol* 2016; 14: 241.
35. Gürsoy ÇA, Uzun Ç, Kul M, *et al.* The impact of arterial phase on the detection of cervical lymph node metastasis from papillary thyroid carcinoma: a quantitative evaluation on multiphase computed tomography. *J Comput Assist Tomogr* 2020; 44: 262–268.
36. Lu W, Zhong L, Dong D, *et al.* Radiomic analysis for preoperative prediction of cervical lymph node metastasis in patients with papillary thyroid carcinoma. *Eur J Radiol* 2019; 118: 231–238.
37. Park JE, Lee JH, Ryu KH, *et al.* Improved diagnostic accuracy using arterial phase CT for lateral cervical lymph node metastasis from papillary thyroid cancer. *Am J Neuroradiol* 2017; 38: 782–788.

Visit SAGE journals online
[journals.sagepub.com/
home/tam](https://journals.sagepub.com/home/tam)

 SAGE journals